A Multisided Generalization of Bézier Surfaces

CHARLES T. LOOP and TONY D. DEROSE
University of Washington

In this paper we introduce a class of surface patch representations, called S-patches, that unify and generalize triangular and tensor product Bézier surfaces by allowing patches to be defined over any convex polygonal domain; hence, S-patches may have any number of boundary curves. Other properties of S-patches are geometrically meaningful control points, separate control over positions and derivatives along boundary curves, and a geometric construction algorithm based on de Casteljau's algorithm. Of special interest are the regular S-patches, that is, S-patches defined on regular domain polygons. Also presented is an algorithm for smoothly joining together these surfaces with C^k continuity.

Categories and Subject Descriptors: I.3.5 [**Computer Graphics**]: Computational Geometry and Object Modeling—*curve, surface, solid, and object representations*; J.6 [**Computer-Aided Engineering**]: *computer-aided design (CAD)*

General Terms: Algorithms

Additional Key Words and Phrases: Computer-aided geometric design, tensor product Bézier surfaces, triangular Bézier surface patches

1. INTRODUCTION

The Bézier curve form was developed independently by P. Bézier and P. de Casteljau in the late 1950s and early 1960s for use in the automotive industry. Since that time, much has been written about the numerous properties of these curves, and the techniques have been effectively applied in many areas of computer-aided geometric design (CAGD). Bézier and de Casteljau also considered extensions of their ideas to surfaces, but the resulting surface forms are quite different. These differences begin with the shape of the domain: de Casteljau's surface has a triangular domain (so-called Bézier triangles), whereas Bézier's surface has a rectangular domain (so-called tensor product Bézier surfaces). Although defined on different domains, the resulting patches are remarkably

This work was supported in part by the National Science Foundation under Grants DMC-8602141 and DMC-8802949, and the Digital Equipment Corporation.
Authors' address: Department of Computer Science, FR-35, University of Washington, Seattle, WA 98195.

similar. Both methods share many interesting and useful properties, including

—the shape of the surface is "intuitively related" to a collection of control points,
—the surface is confined to the convex hull of the control points,
—the shape of the surface is independent of the coordinate system in which the control points are expressed,
—the "corner" control points are interpolated,
—the boundary curves are Bézier curves,
—the mathematical representation of the surface is a parametric polynomial (or possibly rational polynomial), and
—there is a simple geometric algorithm for constructing points lying on the surface.

Despite these similarities, the theory (and implementation) of these techniques have progressed independently.

In this paper we present a theory of surface patches that exposes a deep connection between Bézier triangles and tensor product Bézier surfaces, and extends these techniques to n-sided convex polygonal domains. The unification of Bézier triangles and tensor product surfaces is important from a theoretical perspective because it provides new insight into the similarities possessed by both techniques. It may also prove to be useful from a practical standpoint because it allows both methods to be implemented with a single, more general algorithm. The need for extensions to n-sided domains has been recognized for some time in the CAGD literature (cf. [15] and [27]). Charrot and Gregory pioneered the development of n-sided patches in the spirit of Coons' patches [2, 14–16]. Some work has been done to generalize triangular and tensor product Bézier patches, but the proposed methods impose severe restrictions on the number of sides of the domain polygon [19, 25].

Our method overcomes these limitations while maintaining the properties listed above. However, the polynomial degree and storage requirements for these patches (with boundary curves of comparable degree) increase as a function of n. For instance, a bicubic tensor product Bézier surface requires more storage and is of higher total degree than a cubic Bézier triangle. This, together with the fact that an n-sided patch may be simulated by collections of 3- or 4-sided patches (cf. [3], [11], and [17]), may stir debate over the practicality of true n-sided patches for $n > 4$. It should be pointed out, however, that arguments against the use of true n-sided patches are often *quantitative* (i.e., they appeal to time and space considerations), as opposed to *qualitative* (i.e., which surface is the *fairest*). Others might contend that the inclusion of multiple surface types in a modeling system increases software complexity via a proliferation of special cases. The unifying nature of this work has precisely the opposite effect since only one surface type need be implemented.

Although the ideas will be made more precise in later sections, roughly speaking, our approach is as follows: While Bézier methods (also called Bernstein–Bézier methods) have not previously been generalized to arbitrary domain polygons, they have been generalized to arbitrary dimensions to describe volumes, hypervolumes, and so on. This is accomplished using multivariate Bernstein

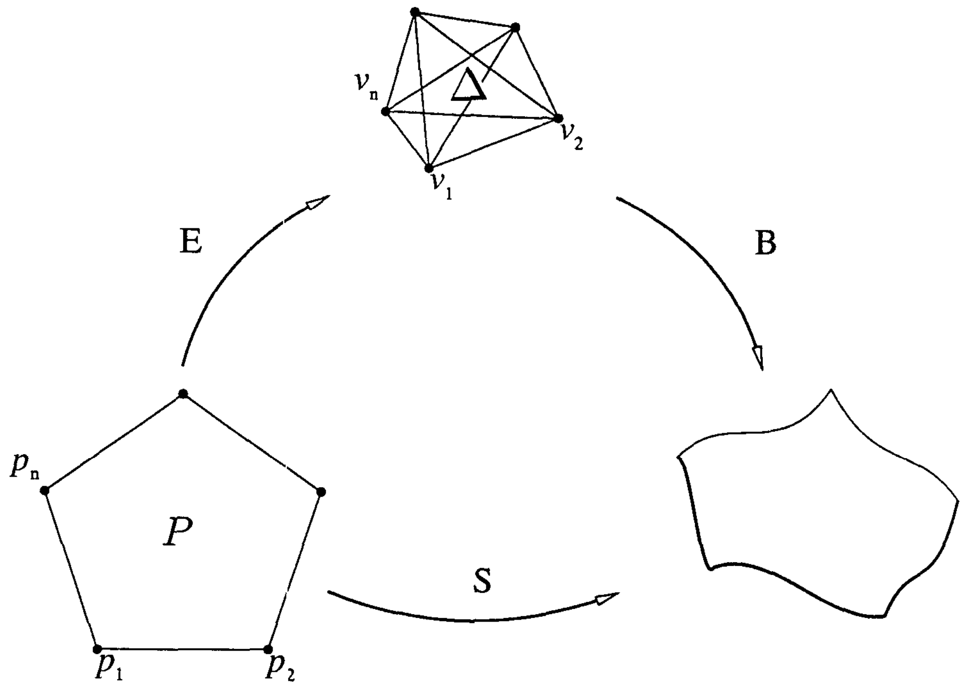

Fig. 1. Schematic representation of S-patches.

polynomials, leading to functions defined on simplexes (a two-dimensional simplex is a triangle, a three-dimensional simplex is a tetrahedron, and so forth for higher dimensions). The theory of the resulting functions, called Bézier simplexes or B-forms, is well developed (cf. [4], [6], and [22]). Conceptually, we construct an n-sided patch S by embedding its n-sided domain polygon P into a simplex Δ whose dimension is one less than the number of sides of the polygon. A Bézier simplex $\mathbf{B}$ is then constructed using Δ as a domain. The patch representation S is obtained by restricting the Bézier simplex to the embedded domain polygon. If E denotes the embedding, the patch representation S can be expressed as a composition

$$S(p) = \mathbf{B} \circ E(p), \qquad p \in P,$$

as indicated in Figure 1. The control net of S is then defined to be the control net of $\mathbf{B}$.

We call these representations "S-patches" to emphasize their connection to the theory of Bézier simplexes. Much of the power of the method is derived from the way in which the domain polygon P is embedded in the simplex Δ. Bézier simplexes have the property that the position and boundary derivatives at the edges of the domain simplex can be controlled individually (cf. [4]). This property is exploited in S-patches by requiring that the embedding of the polygon into the simplex be such that the edges of the polygon map to edges of the simplex. In this way, it is guaranteed that the edges of the polygon map to individually controllable Bézier curves and that a large degree of separation is achieved in controlling boundary derivatives. Higher order derivatives also behave nicely, as is discussed more fully in Section 5.

The separation of boundary control makes S-patch representations potentially attractive tools for CAGD applications, where surface patches of an indeterminate number of sides must be joined together in a smooth fashion. The primary purpose of this paper is to uncover basic S-patch properties and algorithms. We must stress, however, that there remains much to be done and that many fundamental questions are still open, a number of which are summarized in Section 8.

The paper is structured as follows: Background material is presented in Section 2. In Section 3 the basic definitions are presented, and an example of an embedding satisfying our requirements is constructed. In Section 4 we address the issue of how S-patch control nets are represented. In Section 5 many of the fundamental properties of S-patches are enumerated. In Section 6 a particularly useful special case of S-patches, called regular S-patches, is introduced, and in Section 6.1 it is shown that regular 4-sided S-patches are very closely related to tensor product Bézier surfaces. In Section 6.2 a useful property of the regular embedding is identified and proved, and in Section 7 this property is used to develop a geometric algorithm for connecting regular S-patches to Bézier triangles with C^k continuity.

2. BACKGROUND

Readers not proficient in the basic theory of triangular and tensor product Bézier surfaces are encouraged to consult [1], [12], and [13]. An abbreviated account of simple concepts and terminology of affine geometry and Bézier simplexes can be found in [6]. More complete treatments of these topics can be found in [4], [7], and [9]. It is the purpose of this section to familiarize the reader with our notation and with the basic notions of Ramshaw's development of *polar forms* [22, 23]. (Historical note: In [22] and [23], the term *blossom* was used instead of *polar form*. *Polar form* is the currently accepted term so as to conform more closely with classical multilinear algebra [24].)

In what follows, multi-indexes will be denoted by italic characters ornamented with a diacritical arrow, as in $\vec{i}$. For our purposes, multi-indexes are tuples of nonnegative integers, the components of which are subscribed starting at one; for instance, $\vec{i} = (i_1, \ldots, i_n)$.[1] Following Farin, the norm of a multi-index $\vec{i}$, denoted by $|\vec{i}|$, is defined to be the sum of the components of $\vec{i}$. By setting $\vec{i} = (i_1, \ldots, i_{k+1})$ and requiring that $|\vec{i}| = d$, the k-variate Bernstein polynomials of degree d can be defined by

$$B^d_{\vec{i}}(u_1, \ldots, u_{k+1}) = \binom{d}{\vec{i}} u_1^{i_1} u_2^{i_2} \cdots u_{k+1}^{i_{k+1}}$$

where $\binom{d}{\vec{i}}$ is the multinomial coefficient defined by

$$\binom{d}{\vec{i}} = \frac{d!}{i_1!\, i_2! \cdots i_{k+1}!}$$

[1] In many works indexes are chosen to run from 0 to k rather than from 1 to $k + 1$. We have chosen the latter convention because it simplifies later discussions.

and where $u_1, \ldots, u_{k+1}$ are real numbers that sum to one. It is well known that every polynomial $Q: \mathscr{X}_1 \to \mathscr{X}_2$ of degree d, where $\mathscr{X}_1$ is an affine space of dimension k and $\mathscr{X}_2$ is an affine space of arbitrary dimension, can be represented uniquely in Bernstein–Bézier form once a domain simplex δ is chosen in $\mathscr{X}_1$. That is, for every polynomial $Q: \mathscr{X}_1 \to \mathscr{X}_2$, there exist unique points $\mathbf{V}_{\vec{i}}$ in $\mathscr{X}_2$ such that

$$Q(u) = \sum_{\vec{i}} \mathbf{V}_{\vec{i}} B_{\vec{i}}^d(u_1, \ldots, u_{k+1}), \tag{2.1}$$

where $u_1, \ldots, u_{k+1}$ are the barycentric coordinates of u relative to the domain simplex δ. Summations such as the one in eq. (2.1) above are intended to be taken over all multi-indexes whose norm matches the degree of the Bernstein polynomial. Thus, in eq. (2.1), the multi-index $\vec{i}$ is to take on all values such that $|\vec{i}| = d$.

The points $\mathbf{V}_{\vec{i}}$ are individually referred to as control points and collectively referred to as the Bézier control net for Q relative to δ. We shall refer to polynomials represented as in eq. (2.1) as Bézier simplexes; when $k = 2$, we shall refer to such representations as Bézier triangles, and when $k = 3$, we shall refer to such representations as Bézier tetrahedrons.

Ramshaw [22, 23] has recently uncovered a beautiful and powerful connection between Bézier simplexes and symmetric multiaffine maps. (A map $f(u_1, \ldots, u_d)$ is said to be multiaffine if it is affine when all but one of its arguments is held fixed; it is said to be symmetric if its value does not depend on the ordering of the arguments.) Associated with every polynomial $Q: \mathscr{X}_1 \to \mathscr{X}_2$ of degree d there is a unique, symmetric, d-affine map that agrees with Q on its diagonal (the diagonal of a multiaffine function $f(u_1, \ldots, u_d)$ is the function obtained when all arguments are equal: $F(u) = f(u, u, \ldots, u)$). Ramshaw refers to this multiaffine map as the *polarization* of Q. Ramshaw also shows that the Bézier control net for a polynomial relative to a domain simplex can be obtained by evaluating the polynomial's polarization at the vertices of the simplex. More precisely, if $\mathscr{X}_1$ is an affine space of dimension k, if $Q: \mathscr{X}_1 \to \mathscr{X}_2$ is a polynomial of degree d having polarization q, and if $\Delta = (v_1, \ldots, v_{k+1})$ is a simplex in $\mathscr{X}_1$, Ramshaw shows that the Bézier control net of Q relative to Δ is given by

$$\mathbf{V}_{\vec{i}} = q(\overbrace{\underbrace{v_1, \ldots, v_1}_{i_1}, \underbrace{v_2, \ldots, v_2}_{i_2}, \ldots, \underbrace{v_{k+1}, \ldots, v_{k+1}}_{i_{k+1}}}^{d}).$$

Rational polynomial maps can also be described using Bernstein–Bézier methods and polar forms. Rational polynomial maps of degree d can be represented as Bézier simplexes by tagging each of the control vertices with a positive weight. These representations take the form

$$Q(u) = \frac{\sum_{\vec{i}} w_{\vec{i}} \mathbf{V}_{\vec{i}} B_{\vec{i}}^d(u_1, \ldots, u_{k+1})}{\sum_{\vec{j}} w_{\vec{j}} B_{\vec{j}}^d(u_1, \ldots, u_{k+1})}.$$

Associated with each of these representations is a unique, symmetric, d-projective map called its *projective polarization.*

3. BASIC DEFINITIONS

Referring to Figure 1, an n-sided S-patch is obtained by restricting a Bézier simplex of dimension $n - 1$ to a surface obtained by smoothly embedding the n-sided domain polygon P in such a way that edges of the polygon map to edges of an intermediate simplex Δ, and the interior of the polygon maps to the interior of the intermediate simplex. In the remainder of this paper, these ideas are made more precise, and some basic properties of S-patches are identified.

Unless otherwise stated, we use $\mathscr{X}$ to denote the domain space (an affine plane) of an n-sided S-patch S, and we denote by $\mathscr{M}$ the modeling space (i.e., the range of S); we use $P \subset \mathscr{X}$ to denote the convex polygonal domain having vertices $p_1, \ldots, p_n$; we use $\mathscr{Y}$ to denote an affine space of domain $n - 1$; and we use Δ to denote a simplex in $\mathscr{Y}$ having vertices $v_1, \ldots, v_n$ (see Figure 1).

Remark. All indexes are to be interpolated in a cyclic fashion. That is, every index i is to be mapped into the range $1, \ldots, n$ according to $[(i - 1) \bmod n] + 1$.

Definition 3.1. A C^∞ mapping $E: P \to \mathscr{Y}$ is said to be an *edge-preserving* embedding of P into Δ if

(i) p in the interior of P implies that $E(p)$ is in the interior of Δ and
(ii) p on an edge of P implies that $E(p)$ is on an edge of Δ.

We note that every embedding can be written as

$$E(p) = e_1(p)v_1 + \cdots + e_n(p)v_n,$$

where $e_1, \ldots, e_n: P \to \mathbf{R}$ are functions that partition unity and are nonnegative whenever $p \in P$ (a set of functions is said to partition unity if it sums to one at every point of its domain). A simple consequence of the definition is that edge-preserving embeddings must carry vertices in P into vertices in Δ.

We now construct a particularly useful instance of an edge-preserving embedding, which we shall denote by L. (Throughout the remainder of this paper, the symbol E will be used to represent an arbitrary edge-preserving embedding, whereas the symbol L shall refer to the particular edge-preserving embedding that follows.)

Let $\alpha_i(p)$ denote the ratio of the signed area of the triangle pp_ip_{i+1} to the area of the triangle $p_ip_{i+1}p_{i+2}$, as shown in Figure 2, where the sign is chosen to be positive if p is inside P. Let $\pi_i(p)$ denote the product of all αs, except for $\alpha_{i-1}(p)$ and $\alpha_i(p)$; that is,

$$\pi_i(p) = \alpha_1(p) \cdots \alpha_{i-2}(p)\, \alpha_{i+1}(p) \cdots \alpha_n(p), \qquad i = 1, \ldots, n;$$

and let

$$l_i(p) = \frac{\pi_i(p)}{\pi_1(p) + \cdots + \pi_n(p)}, \qquad i = 1, \ldots, n.$$

Remark. For those concerned about the use of Euclidean concepts in the definitions above, it should be noted that since α_i is defined in terms of ratios of areas it is actually an affinely invariant function. In fact, a strict affine definition is "$\alpha_i: P \to \mathbf{R}$ is the unique affine function that vanishes at p_i and p_{i+1} and achieves the value 1 at p_{i+2}." A more symmetric definition would have the

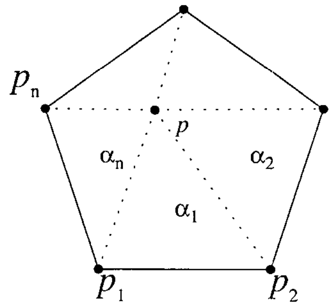

Fig. 2. Geometry of the affine functions used to construct the embedding L.

function achieve a value $\frac{1}{n}$ at the centroid of P. We use the former definition to simplify subsequent proofs.

By construction, the functions $l_1, \ldots, l_n$ form a partition of unity and are rational polynomial functions of degree $n - 2$. Moreover, they are guaranteed to be nonnegative whenever $p \in P$ since each of the functions α_i are nonnegative in this case.

Example 3.1. Consider the construction of the embedding L for the pentagonal case. The normalized area functions $\alpha_i(p)$ may be defined as

$$\alpha_i(p) = \kappa \det\begin{pmatrix} p^u & p_i^u & p_{i+1}^u \\ p^v & p_i^v & p_{i+1}^v \\ 1 & 1 & 1 \end{pmatrix}, \tag{3.1}$$

where κ is a normalization constant that need not be computed, and superscripts u and v denote coordinates with respect to some coordinate system on the domain $\mathscr{X}$. The functions $\pi_i(p)$ for $i = 1, \ldots, 5$ are defined as

$$\begin{aligned} \pi_1(p) &= \alpha_2(p)\alpha_3(p)\alpha_4(p), \\ \pi_2(p) &= \alpha_3(p)\alpha_4(p)\alpha_5(p), \\ \pi_3(p) &= \alpha_4(p)\alpha_5(p)\alpha_1(p), \\ \pi_4(p) &= \alpha_5(p)\alpha_1(p)\alpha_2(p), \\ \pi_5(p) &= \alpha_1(p)\alpha_2(p)\alpha_3(p). \end{aligned} \tag{3.2}$$

Finally, the functions $l_i(p)$ for $i = 1, \ldots, 5$ are defined as

$$\begin{aligned} l_1(p) &= \frac{\pi_1(p)}{\pi_1(p) + \pi_2(p) + \pi_3(p) + \pi_4(p) + \pi_5(p)}, \\ l_2(p) &= \frac{\pi_2(p)}{\pi_1(p) + \pi_2(p) + \pi_3(p) + \pi_4(p) + \pi_5(p)}, \\ l_3(p) &= \frac{\pi_3(p)}{\pi_1(p) + \pi_2(p) + \pi_3(p) + \pi_4(p) + \pi_5(p)}, \\ l_4(p) &= \frac{\pi_4(p)}{\pi_1(p) + \pi_2(p) + \pi_3(p) + \pi_4(p) + \pi_5(p)}, \\ l_5(p) &= \frac{\pi_5(p)}{\pi_1(p) + \pi_2(p) + \pi_3(p) + \pi_4(p) + \pi_5(p)}. \end{aligned} \tag{3.3}$$

For a coordinate definition of (3.3), (3.1) may be expanded and substituted in (3.2) and (3.3). This is rather cumbersome to do by hand, but very easy to program.

Since the functions $l_1, \ldots, l_n$ partition unity and are nonnegative whenever p is inside the domain polygon, the embedding $L: P \rightarrow \Delta$ given by

$$L(p) = l_1(p)v_1 + \cdots + l_n(p)v_n, \qquad p \in P, \tag{3.4}$$

maps the interior of the polygon P into the interior of the simplex Δ. To show that L is actually edge-preserving, let p_e be a point on the edge p_1p_2. In this case, the function α_1 vanishes, implying that all l_is vanish except for l_1 and l_2 since these are the only two that do not contain α_1 (cf. eqs. (3.2) and (3.3)). Thus, $L(p_e)$ can be written as

$$L(p_e) = l_1(p_e)v_1 + l_2(p_e)v_2, \tag{3.5}$$

which is clearly a point on the v_1v_2 edge of Δ, showing that the p_1p_2 edge of P maps to the v_1v_2 edge of Δ, for all $i = 1 \cdots n$. By symmetry, the edge p_ip_{i+1} of P is mapped to the v_iv_{i+1} edge of Δ.

It is interesting to note that the functions $l_1, \ldots, l_n$ are actually a generalization of barycentric coordinates. Taking $n = 3$, we find that

$$l_1(p) = \frac{\alpha_2(p)}{\alpha_1(p) + \alpha_2(p) + \alpha_3(p)}.$$

The denominator is an affine function that has value 1 at the vertices p_1, p_2, and p_3—it must therefore be identically 1. Thus, $l_1(p) = \alpha_2(p)$, implying that l_1 is the unique affine function that vanishes at p_2 and p_3, and attains the value 1 at p_1. Since these are exactly the defining characteristics of barycentric coordinates, l_1 must be a barycentric coordinate function; a symmetric argument holds for l_2 and l_3. The affine nature of l_1, l_2, l_3 means that L is simply an affine map from $p_1p_2p_3$ onto $v_1v_2v_3$.

The behavior of the functions $l_i(p)$ for various values of n is illustrated in the contour plots of Figure 3. These plots empirically demonstrate the edge-preserving character of the functions.

Before returning to the case of a general edge-preserving embedding E, we should point out that functions $l_1, \ldots, l_n$ are not new to CAGD. Herron [17] and Charrot and Gregory [2] discuss equivalent formulations in connection with n-sided convex combination surface schemes.

We are now in a position to rigorously define the class of S-patch surfaces:

Definition 3.2. An n-sided S-patch of depth d is a map $S: P \rightarrow \mathscr{M}$ of the form $S = \mathbf{B} \circ E$, where $E: P \rightarrow \Delta$ is an edge-preserving embedding of P into Δ and $\mathbf{B}: \Delta \rightarrow \mathscr{M}$ is a rational Bézier simplex of degree d, expressed relative to the domain simplex Δ.

We use the word *depth* in the definition of S-patches to avoid confusion with the rational polynomial degree of the patch itself. In fact, depending on the functional form of the embedding E, S may not even be a rational polynomial map. However, if the map L from eq. (3.4) is used as the embedding, then the S-patch will be a rational polynomial surface whose degree is the product of

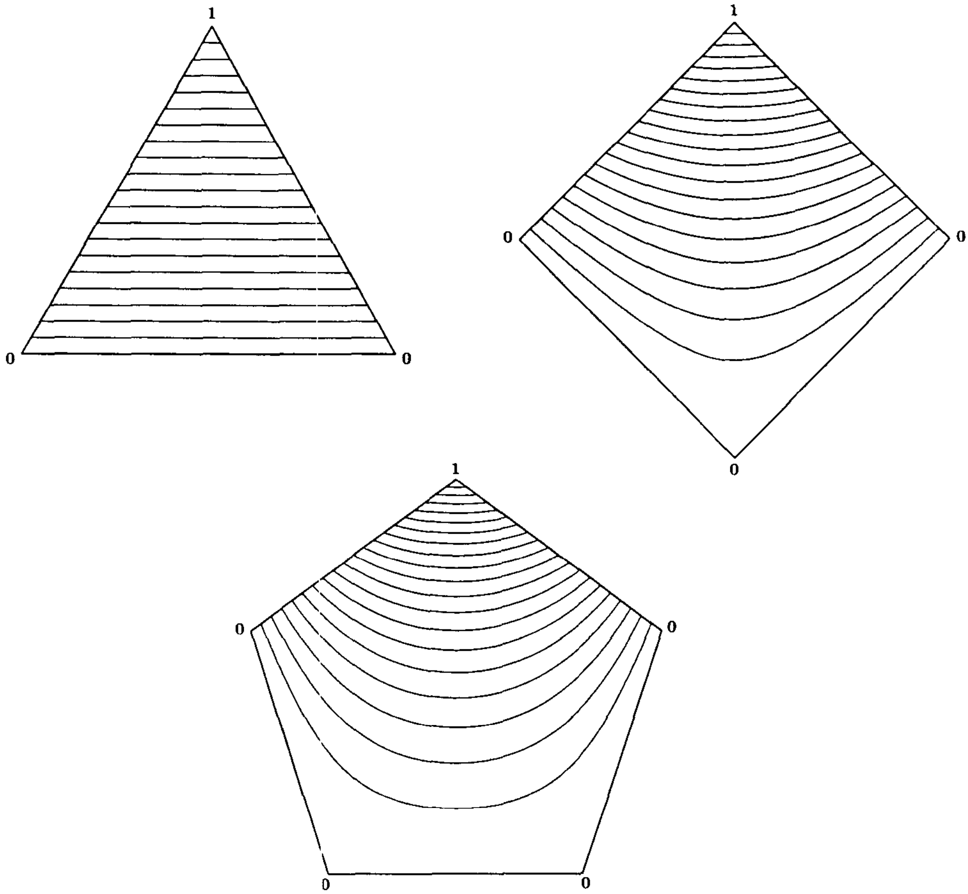

Fig. 3. Contour plots of the functions $l_i(p)$ from eq. (3.4). Contours are drawn every $\frac{1}{20}$ of a unit.

the degrees of **B** and L. Thus, when L is used as the embedding, an n-sided S-patch of depth d is of rational degree $d(n-2)$.

Just as the domain triangle of a Bézier triangle does not affect the shape of the resulting patch, the simplex Δ does not affect the shape of an S-patch. This is most easily seen by writing S as

$$S(p) = \frac{\sum_{\vec{i}} w_{\vec{i}} \mathbf{V}_{\vec{i}} B^d_{\vec{i}}(e_1(p), \ldots, e_n(p))}{\sum_{\vec{j}} w_{\vec{j}} B^d_{\vec{i}}(e_1(p), \ldots, e_n(p))}, \qquad p \in P, \tag{3.6}$$

where

—$\mathbf{V}_{\vec{i}}$ are the S-patch control points for S relative to P;
—$w_{\vec{i}}$ is the rational weight associated with the control point $\mathbf{V}_{\vec{i}}$; and
—$(e_1(p), \ldots, e_n(p))$ are the barycentric coordinates of $E(p)$ relative to Δ.

Equation (3.6) also points out that the shape of S is controlled by manipulating the control net $\mathbf{V}_{\vec{i}}$ and the weights $w_{\vec{i}}$. Equation (3.6) can also be used to define

S-patch blending functions. Specifically, eq. (3.6) can be rewritten as

$$S(p) = \sum_{\vec{i}} \mathbf{V}_{\vec{i}} W_{\vec{i}}^d(p), \qquad p \in P,$$

where

$$W_{\vec{i}}^d(p) = \frac{w_{\vec{i}} B_{\vec{i}}^d(e_1(p), \ldots, e_n(p))}{\sum_{\vec{j}} w_{\vec{j}} B_{\vec{j}}^d(e_1(p), \ldots, e_n(p))},$$

is defined to be the $\vec{i}$th S-patch blending function of depth d.

Alternatively, S = path blending functions may be found by forming a multinomial expansion of the embedding component functions (the e_is) and grouping like monomial terms. Since

$$1 = e_1(p) + e_2(p) + \cdots + e_n(p),$$

it follows that

$$\begin{aligned} 1 &= (e_1(p) + e_2(p) + \cdots + e_n(p))^d \\ &= \sum_{\vec{i}} \binom{d}{\vec{i}} e(p)_1^{i_1} e(p)_2^{i_2} \cdots e(p)_n^{i_n}, \end{aligned} \tag{3.7}$$

from the multinomial theorem. The terms of (3.7) are S-patch blending functions with rational weights $w_{\vec{i}} = 1$; that is,

$$W_{\vec{i}}^d(p) = \binom{d}{\vec{i}} e(p)_1^{i_1} e(p)_2^{i_2} \cdots e(p)_n^{i_n}.$$

Example 3.2. As a specific example, consider the construction of S-patch blending functions using the embedding L for the case $n = 5$ and $d = 2$, with all rational weights set to 1. From (3.7), the complete set of blending functions are

$$\begin{array}{lll}
W^2_{(2,0,0,0,0)}(p) = l_1(p)^2, & W^2_{(1,1,0,0,0)}(p) = 2l_1(p)l_2(p), & W^2_{(1,0,1,0,0)}(p) = 2l_1(p)l_3(p), \\
W^2_{(1,0,0,1,0)}(p) = 2l_1(p)l_4(p), & W^2_{(1,0,0,0,1)}(p) = 2l_1(p)l_5(p), & W^2_{(0,2,0,0,0)}(p) = l_2(p)^2, \\
W^2_{(0,1,1,0,0)}(p) = 2l_2(p)l_3(p), & W^2_{(0,1,0,1,0)}(p) = 2l_2(p)l_4(p), & W^2_{(0,1,0,0,1)}(p) = 2l_2(p)l_5(p), \\
W^2_{(0,0,2,0,0)}(p) = l_3(p)^2, & W^2_{(0,0,1,1,0)}(p) = 2l_3(p)l_4(p), & W^2_{(0,0,1,0,1)}(p) = 2l_3(p)l_5(p), \\
W^2_{(0,0,0,2,0)}(p) = l_4(p)^2, & W^2_{(0,0,0,1,1)}(p) = 2l_4(p)l_5(p), & W^2_{(0,0,0,0,2)}(p) = l_5(p)^2.
\end{array}$$

4. CONTROL NETS

The shapes of S-patches are intuitively related to their control nets, at least when L is used as the embedding. It is therefore convenient to describe how S-patch control nets are depicted graphically.

Since the control net of an S-patch is the control net of a Bézier simplex, S-patch control nets could be drawn in the same way that control nets for Bézier simplexes are drawn. For example, the control net for a 4-sided S-patch could be drawn as a control net for a Bézier tetrahedron, as shown in Figure 4a.

Although the position of the points in the net is crucial, the connectivity of the points is somewhat arbitrary. In particular, when drawing control nets for Bézier simplexes the usual rule for connecting points $\mathbf{V}_{\vec{i}}$ and $\mathbf{V}_{\vec{j}}$ is that there

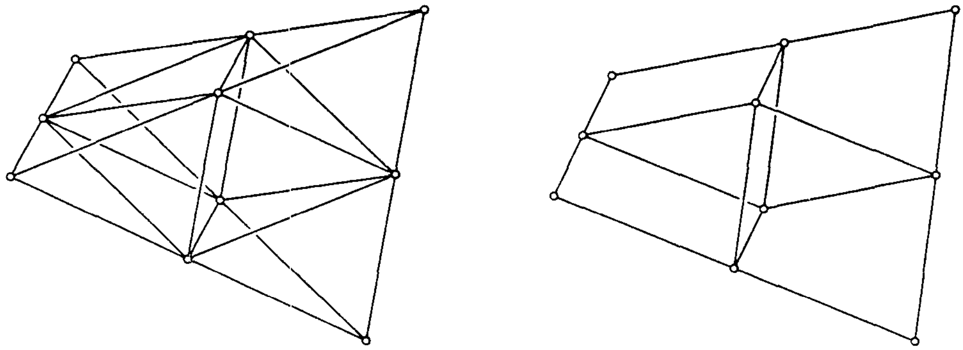

(a) (b)

Fig. 4. (a) The control net for a Bézier tetrahedron; (b) the S-patch control net obtained by using the connectivity rule given in eq. (4.2).

must exist integers r and s such that the multi-indexes $\vec{i}$ and $\vec{j}$ satisfy

$$\vec{i} - \vec{e}_s = \vec{j} - \vec{e}_r, \tag{4.1}$$

where $\vec{e}_\alpha$ denotes the multi-index having zeros in all components except for the αth component, which is one. This connectivity rule is appropriate for Bézier simplexes since it reflects the fact that the domain simplex has all vertices connected to all other vertices. This reflects the fact that there is no natural ordering on the vertices of the simplex.

However, for S-patches there is a natural ordering on the vertices in the domain polygon. Since E must carry vertices in P into vertices in Δ, a natural ordering on the vertices in Δ is imposed. The ordering can be reflected in the depiction of the control net by modifying the connectivity rule. The rule we shall use is that $\mathbf{V}_{\vec{i}}$ and $\mathbf{V}_{\vec{j}}$ are connected if there exists an integer r such that

$$\vec{i} - \vec{e}_r = \vec{j} - \vec{e}_{r\pm1}. \tag{4.2}$$

Examples of control nets using this rule are shown in Figures 4b, 5, and 6. A detailed labeling of the control points appropriate for Example 3.2 is shown in Figure 7.

5. GENERAL PROPERTIES

The compositional structure of S-patches allows many of their properties to be immediately deduced from corresponding properties of Bézier simplexes. Below, we list several such properties.

5.1 Geometric Construction Algorithm

The point $S(p)$ can be evaluated by first evaluating $E(p)$, and then evaluating $\mathbf{B}$ at the point $E(p)$ using de Casteljau's algorithm. The fact that de Casteljau's algorithm has an elegant geometric interpretation provides a geometric construction for points on S-patches, as shown in Figure 8.

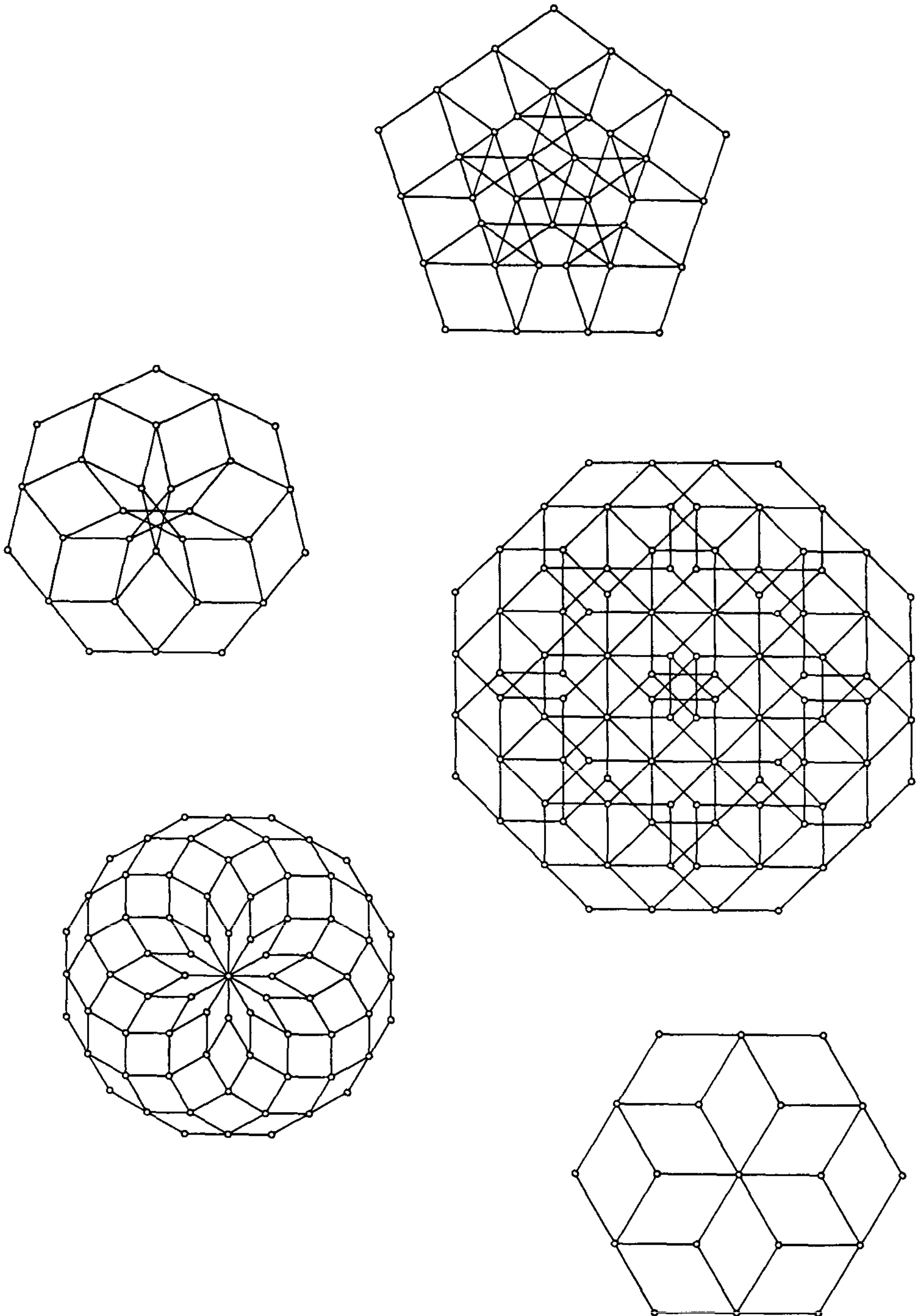

Fig. 5. Examples of S-patch control nets for various numbers of sides and depths.

Fig. 6. Depth 2 S-patches and control nets for 3, 4, and 5 sides.

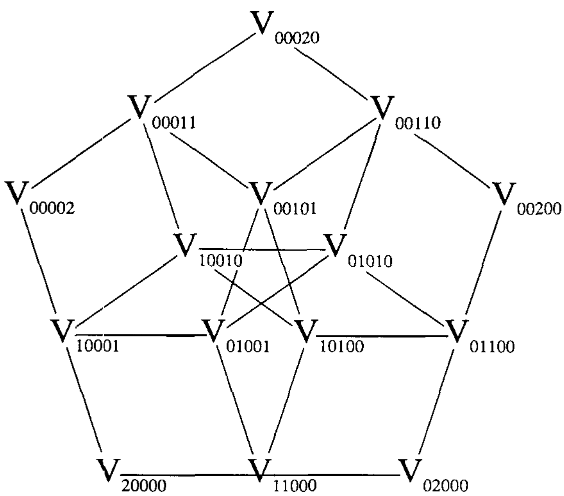

Fig. 7. Labeling of control points for a 5-sided S-patch of depth 2.

5.2 Convex Hull

S-patch surfaces are confined to the convex hull of their control nets. This is a direct consequence of two simple facts: (1) Edge-preserving embeddings map the interior of the domain polygon ***P*** into the interior of the intermediate simplex A, and (2) Bézier simplexes are confined to the convex hull of their control nets.

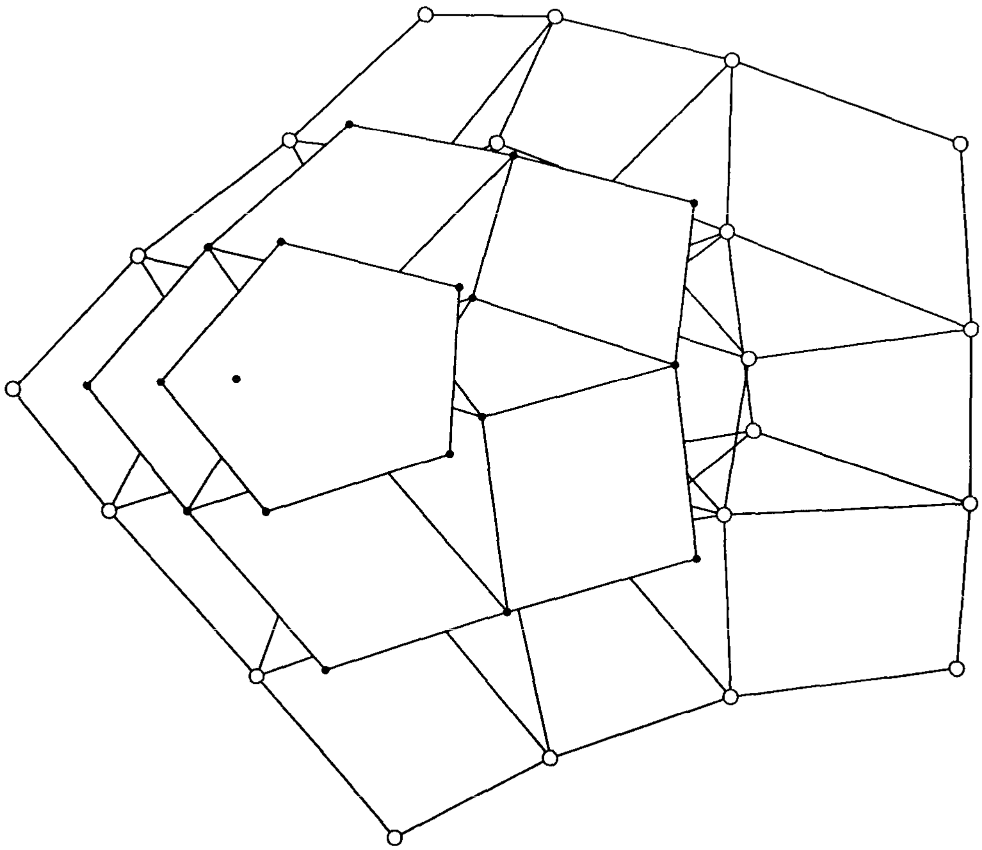

Fig. 8. The S-patch geometric construction algorithm.

5.3 Depth Elevation

Another property possessed by S-patches that is directly inherited from Bézier simplexes is an algorithm for depth elevation. That is, given an S-patch control net of depth d describing a surface $S = \mathbf{B} \circ E$, the S-patch control net of depth $d + 1$ for S can be constructed by using the Bézier simplex degree elevation algorithm on the control net of $\mathbf{B}$ (cf. [4] and [22]).

Repeated degree elevation of a Bézier simplex produces control nets that converge to the image simplex. The implication for S-patches is that repeated depth elevation produces control nets that converge to the image of Δ; they *do not*, in general, converge to the surface patch, except when $n = 3$.

5.4 Boundary Behavior

Perhaps the most important properties of S-patches stem from their behavior along the boundary curves. First, we note that each of the n boundary curves of an S-patch of depth d are rational Bézier curves of degree d defined by the control points associated with the boundary. (An example of this behavior is shown in Figure 6 for the case of depth 2 S-patches of 3, 4, and 5 sides.) This follows from the fact that the edges of the domain polygon map to edges of the simplex, which in turn map to rational Bézier curves under **B** (cf. [4]). Moreover, if the rational weights associated with the boundary control points are equal, the resulting S-patch will have purely polynomial Bézier curves as boundaries. Note that this occurs even if the embedding is not a polynomial or rational polynomial map. Thus, S-patches automatically achieve separation of boundary curve behavior in that only a few control points determine each of the boundary curves. It is therefore trivial to insert an S-patch into a network of, say, Bézier triangles or tensor products in a C^0 fashion (as long as the degree of the triangles or tensor products does not exceed the depth of the S-patch).

Not only do S-patches enjoy separation of positional behavior along the boundary curves, they also exhibit separation of derivative control along the boundaries. For instance, first-order derivatives along a boundary curve are completely determined by the boundary vertices and the vertices adjacent to them (using the usual Bézier simplex connectivity rule of eq. (4.1)). Again, this follows immediately from the fact that the S-patch is obtained by restriction of a Bézier simplex to an embedded surface. Higher order derivatives behave similarly: The rth-order derivative behavior along a boundary curve is determined completely by the vertices a "distance" r or less from the boundary vertices. The term *distance* here refers to the number of edges of the control net that are traversed in a path from a boundary control point (using the Bézier simplex connectivity rule of eq. (4.1)).

6. REGULAR S-PATCHES

By a regular S-patch, we mean an S-patch $S = \mathbf{B} \circ L$, where L is the embedding of eq. (3.4) and S is defined on a domain polygon that is the affine image of a regular n-gon (we call such polygons *regular*). Several interesting phenomena appear when L is used on a regular domain polygon.

The first occurs when $n = 3$, that is, for triangular domains. In this case, L is an affine map, implying that the image of $S = \mathbf{B} \circ L$ is the same as the image of **B**. Thus, S is simply a rational Bézier triangle. In other words, regular S-patches generalize rational Bézier triangles.

The second interesting thing occurs when $n = 4$, that is, for parallelogram domains. In Section 6.1 it is shown that, when the domain is a parallelogram, S-patches generalize rational bi-d-ic tensor product Bézier surfaces.

Remark. Since regular S-patches generalize both the Bézier triangles and the bi-d-ic tensor product Bézier surfaces, the theory of regular S-patches can be used to unify the theories of Bézier triangles and tensor products. For instance, in Section 6.4 we derive an algorithm for representing an m-sided regular S-patch as an n-sided regular S-patch. Unification implies that this algorithm is both an algorithm for converting Bézier triangles into tensor product form (set $m = 3$ and $n = 4$) and an algorithm for converting tensor product surfaces into Bézier triangle form (set $m = 4$ and $n = 3$). Unification also shows that the de Casteljau algorithms for Bézier triangles and tensor product surfaces are specific manifestations of a common, more general construction.

The third interesting thing that occurs for regular S-patches concerns a special property of L. In general, L is a rational polynomial mapping. However, when

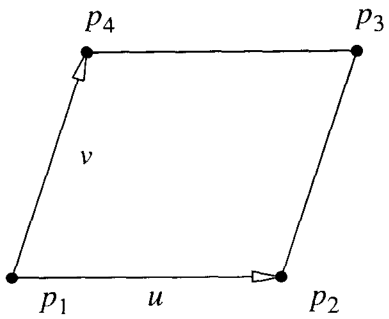

Fig. 9. The domain of a regular 4-sided S-patch.

the domain polygon is regular, L has, in a sense to be precisely defined in Section 6.2, an extremely simple inverse. This fact has striking practical implications. In particular, it is the key to a construction for joining regular S-patches to Bézier triangles and tensor product Bézier surfaces with C^k continuity.

6.1 Regular 4-Sided S-Patches and Tensor Product Surfaces

To investigate the relationship between regular 4-sided S-patches and tensor product surfaces, we establish a coordinate system in the domain space $\mathscr{X}$ by placing the origin at p_1, choosing the unit vector in the u direction to be $p_2 - p_1$, and the unit vector in the v direction to be $p_4 - p_1$, as shown in Figure 9. The representations of the functions $\alpha_1, \ldots, \alpha_4$ in this system are particularly simple. Referring to Figure 9, if p has coordinates (u, v) in this system, then

$$\begin{aligned}\alpha_1(p) &= v\\ \alpha_2(p) &= 1 - u\\ \alpha_3(p) &= 1 - v\\ \alpha_4(p) &= u.\end{aligned}$$

These representations give rise to functions $l_1, \ldots, l_4$ that are also simply expressed. In fact, the common denominator of these functions is identically one:

$$\begin{aligned}&\pi_1(p) + \pi_2(p) + \pi_3(p) + \pi_4(p)\\ &= v(1 - u) + (1 - u)(1 - v) + (1 - v)u + uv = 1.\end{aligned}$$

Thus, the functions $l_1, \ldots, l_4$ become

$$\begin{aligned}l_1(p) &= (1 - u)(1 - v)\\ l_2(p) &= u(1 - v)\\ l_3(p) &= uv\\ l_4(p) &= (1 - u)v.\end{aligned}$$

The simple product structure of these expressions shows a connection to tensor product blending functions. The precise nature of this connection is established in the following lemma:

LEMMA 6.1. *Let p be a point having coordinates (u, v) in the coordinate system of Figure 9, and let $\vec{i} = (i_1, i_2, i_3, i_4)$ be such that $|\vec{i}| = d$. Then*

$$B_{\vec{i}}^d \circ L(p) = \frac{\binom{d}{\vec{i}}}{\binom{d}{i_2 + i_3}\binom{d}{i_3 + i_4}} B_{i_2+i_3}^d(u) B_{i_3+i_4}^d(v).$$

PROOF

$$\begin{aligned} B_{\vec{i}}^d \circ L(p) &= B_{\vec{i}}^d(l_1(p), l_2(p), l_3(p), l_4(p)) \\ &= B_{\vec{i}}^d((1-u)(1-v), u(1-v), uv, (1-u)v) \\ &= \binom{d}{\vec{i}} (1-u)^{i_1}(1-v)^{i_1} u^{i_2}(1-v)^{i_2} u^{i_3} v^{i_3} (1-u)^{i_4} v^{i_4} \\ &= \frac{\binom{d}{\vec{i}}}{\binom{d}{i_2 + i_3}\binom{d}{i_3 + i_4}} \binom{d}{i_2 + i_3}\binom{d}{i_3 + i_4} u^{i_2+i_3}(1-u)^{i_1+i_4} v^{i_3+i_4}(1-v)^{i_1+i_2} \\ &= \frac{\binom{d}{\vec{i}}}{\binom{d}{i_2 + i_3}\binom{d}{i_3 + i_4}} B_{i_2+i_3}^d(u) B_{i_3+i_4}^d(v). \end{aligned}$$

□

An immediate consequence of Lemma 6.1 is that the regular S-patch blending functions are not always linearly independent. As a specific instance, Lemma 6.1 shows that

$$W_{(1,0,1,0)}^2(p) = W_{(0,1,0,1)}^2(p).$$

For practical design applications, it is necessary for blending functions to be independent, so the question of exactly when S-patch blending functions are dependent is an important one. Although the general question is currently open, it is interesting to note that the dependence of the blending functions in the $n = 4$ case is precisely what is needed to establish a connection between S-patches and tensor product surfaces, as the next lemma shows:

LEMMA 6.2. *Let S be a regular 4-sided S-patch of depth d having control points $\mathbf{V}_{\vec{i}}$ and rational weights $w_{\vec{i}} = 1$. S can be written as the following (nonrational) bi-d-ic tensor product surface:*

$$S(p) = \sum_{i,j} \mathbf{W}_{i,j} B_i^d(u) B_j^d(v),$$

where p has coordinates (u, v) relative to the coordinate system of Figure 9 and where

$$\mathbf{W}_{i,j} = \sum_{\substack{\vec{i} \\ i_2+i_3=i \\ i_3+i_4=j}} \frac{\binom{d}{\vec{i}}}{\binom{d}{i}\binom{d}{j}} \mathbf{V}_{\vec{i}}.$$

PROOF

$$S(p) = \sum_{\vec{i}} \mathbf{V}_{\vec{i}} B^d_{\vec{i}} \circ L(p)$$

$$= \sum_{\vec{i}} \mathbf{V}_{\vec{i}} \frac{\binom{d}{\vec{i}}}{\binom{d}{i_2+i_3}\binom{d}{i_3+i_4}} B^d_{i_2+i_3}(u) B^d_{i_3+i_4}(v)$$

$$= \sum_{i,j} \sum_{\substack{\vec{i} \\ i_2+i_3=i \\ i_3+i_4=j}} \frac{\binom{d}{\vec{i}}}{\binom{d}{i_2+i_3}\binom{d}{i_3+i_4}} \mathbf{V}_{\vec{i}} \quad B^d_i(u) B^d_j(v)$$

$$= \sum_{i,j} \mathbf{W}_{i,j} B^d_i(u) B^d_j(v).$$ □

Remark. A slight generalization shows that Lemma 6.2 holds for rational bi-d-ic tensor product Bézier surfaces.

Lemma 6.2 provides a simple algorithm for converting a regular 4-sided S-patch into tensor product form. It also shows that, if each of the S-patch control points $\mathbf{V}_{\vec{i}}$, for all $\vec{i}$ such that $i_2 + i_3 = i$ and $i_3 + i_4 = j$, coincide at a point $\mathbf{W}_{i,j}$, then the S-patch control net is identical to the tensor product control net. In other words, regular 4-sided S-patches generalize bi-d-ic tensor product Bézier surfaces. In order to represent a general r-by-s tensor product surface (i.e., one that is degree r in u and degree s in v, where $r \neq s$), the S-patch must be of depth $\max(r, s)$.

6.2 The Pseudoaffine Property

In the introduction to Section 6, it is claimed that the embedding L possesses a certain property when the domain polygon P is regular. The property of interest is a generalization of a property satisfied by barycentric coordinates for triangles. The definition of barycentric coordinates for triangles associates with each point p in a triangle $p_1p_2p_3$ a triple of numbers β_1, β_2, β_3 that partition unity and are such that

$$p = \beta_1 p_1 + \beta_2 p_2 + \beta_3 p_3.$$

More generally, the embedding L associates with each point p in an n-gon $p_1, \ldots, p_n$ a collection of numbers $l_1(p), \ldots, l_n(p)$. In order to generalize barycentric coordinates as closely as possible, we would like the l_is to be such that

$$p = l_1(p)p_1 + \cdots + l_n(p)p_n. \tag{6.1}$$

Loosely speaking, when this relation holds, we say that L possesses the pseudoaffine property (motivation for this term will be explained shortly). Although L does not possess the pseudoaffine property for arbitrary n-gons, in the appendix it is shown that L does possess it when the n-gon is regular. Rather than defining pseudoaffineness by making explicit reference to components of L (the l_is), we shall find it more convenient for later use to phrase pseudoaffineness for arbitrary maps without reference to the components of the map.

Definition 6.1. Let $M: \mathscr{X}_1 \to \mathscr{X}_2$ be any map from an affine space $\mathscr{X}_1$ into an affine space $\mathscr{X}_2$. M is said to be *pseudoaffine* if there exists an affine map F: $\mathscr{X}_2 \to \mathscr{X}_1$ such that $F \circ M$ is the identity map on $\mathscr{X}_1$. When such a map F exists, we say that M is pseudoaffine with respect to F.

The term *pseudoaffine* is motivated by the fact that, if a map M is pseudoaffine, then, even if M is itself nonaffine, it has a left inverse that is affine. Intuitively speaking, a map is pseudoaffine if its nonaffine behavior can be affinely "projected out." In the appendix the following claim is proved, showing that the embedding L is such a map whenever the domain polygon is regular:

CLAIM 6.1. *Let* $A: \mathscr{Y} \dashrightarrow \mathscr{X}$ *be the unique affine map that carries* v_i *into* p_i *for* $i = 1, \ldots, n$. *The embedding* $L: P \to \mathscr{Y}$ *is pseudoaffine with respect to* A *whenever* P *is regular.*

PROOF. See Appendix A. □

It is the pseudoaffine property that allows polynomial functions to be represented in S-patch form. This has a number of useful consequences: It allows Bézier triangles to be represented as n-sided S-patches (see Section 6.4), it allows the graphs of scalar valued functions to be represented as S-patches (see Section 6.5), and it allows S-patches to inherit algorithms for connecting Bézier triangles with geometric continuity (see Section 7).

6.3 Subdivision

Subdivision algorithms are among the most powerful techniques currrently used in CAGD. It is therefore natural to study the character of subdivision algorithms for S-patches. Unfortunately, it is rather unlikely that such algorithms exist, at least in the usual sense. To investigate this further, we note that a subdivision algorithm for regular S-patches would typically be characterized as follows:

Given. A control net for an n-sided S-patch S of depth d defined on an n-gon P. Also input to the problem is another n-gon P'.

Find. The control net for an n-sided S-patch of depth d defined on P' that exactly reproduces S.

If an algorithm existed to solve this problem, then the fact that S-patch boundaries are Bézier curves implies that the images of the edges of P' are curves

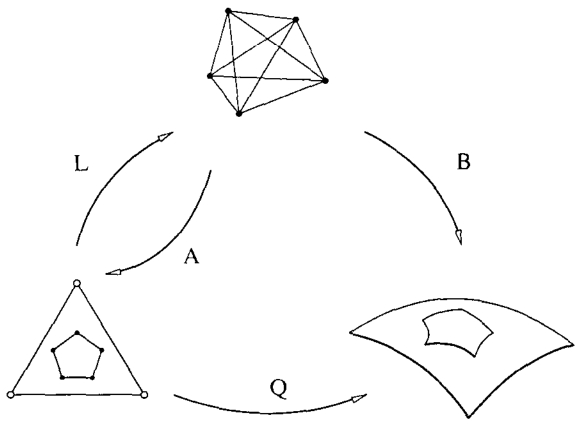

Fig. 10. The geometric interpretation of eq. (6.2).

of degree d. However, in general, the image of a line on an n-sided S-patch of depth d is a rational curve of degree $d(n-2)$. Thus, if an algorithm exists at all, it cannot exist for an arbitrary polygon P'. Tensor product surfaces provide an example of a technique where subdivision does not exist for arbitrary P', but does exist for specially chosen ones (P' must be a parallelogram whose sides are parallel to the sides of P). If special polygons P' exist for general S-patches, we have yet to identify them.

6.4 Representation Theorems

In this section we show that the space of bivariate polynomials of degree d is contained in the span of regular n-sided S-patches of depth d, for all $n \geq 3$. We then derive an algorithm for the construction of an S-patch control net for a given polynomial. As a consequence of the pseudoaffine behavior of L, the S-patch control net for a polynomial Q is shown to be intimately related to the theory of polar forms in that the S-patch control points correspond to certain values of Q's polarization.

CLAIM 6.2. *The space of bivariate polynomials of degree d is contained in the space of regular n-sided S-patches of depth d.*

PROOF. Let $Q: \mathscr{X} \to \mathscr{M}$ denote an arbitrary bivariate polynomial of degree d for which the existence of an S-patch representation is to be demonstrated, and let $A: \mathscr{Y} \to \mathscr{X}$ be the affine map that carries v_i into p_i for all i.

Recall that A as defined above is such that, as a consequence of Claim 6.1, the map $A \circ L: \mathscr{X} \to \mathscr{X}$ is the identity map I of $\mathscr{X}$ onto itself. The key to the proof (and the algorithm) is as follows, the geometric interpretation of which is shown in Figure 10:

$$\begin{aligned} Q &= Q \circ I \\ &= Q \circ (A \circ L) \\ &= (Q \circ A) \circ L \\ &= \mathbf{B} \circ L. \end{aligned} \tag{6.2}$$

Since $\mathbf{B} = Q \circ A: \Delta \rightarrow \mathcal{M}$ is a composition of purely polynomial maps, $\mathbf{B}$ is itself a purely polynomial map; thus, Q written as $Q = \mathbf{B} \circ L$ is a map in regular S-patch form. The S-patch control net of Q is the control net of $\mathbf{B}$, the construction of which is described in Claim 6.3. □

CLAIM 6.3. *Let $Q: \mathcal{X} \rightarrow \mathcal{M}$ be a polynomial of degree d having polarization q. The regular S-patch representation of depth d for Q on the (regular) polygon $p_1, \ldots, p_n$* has control points given by

$$\mathbf{V}_{\vec{i}} = q(\underbrace{p_1, \ldots, p_1}_{i_1}, \underbrace{p_2, \ldots, p_2}_{i_2}, \ldots, \underbrace{p_n, \ldots, p_n}_{i_n}),$$

with rational weights that are all equal to unity.

PROOF. The proof is actually a special case of Claim 4.3 of [6]. Here we offer an alternative proof tailored to the special case that is substantially shorter and more to the point.

From the proof of Claim 6.2, the S-patch control net of Q is the control net of the composition map $\mathbf{B} := Q \circ A$, where A is the affine map carrying v_i onto p_i, $i = 1, \ldots, n$. This control net can be determined by appropriate evaluation of the polarization $\mathbf{b}$ of $\mathbf{B}$. The polarization $\mathbf{b}$ can be written as

$$\mathbf{b}(u_1, \ldots, u_d) = q(A(u_1), \ldots, A(u_d))$$

since this is the unique symmetric d-affine function whose diagonal agrees with $\mathbf{B}$. Evaluating $\mathbf{b}$ at the vertices of the simplex Δ yields $\mathbf{B}$'s control net and, hence, the S-patch control net for Q:

$$\begin{aligned}\mathbf{V}_{\vec{i}} &= \mathbf{b}(\underbrace{v_1, \ldots, v_1}_{i_1}, \underbrace{v_2, \ldots, v_2}_{i_2}, \ldots, \underbrace{v_n, \ldots, v_n}_{i_n}) \\ &= q(\underbrace{A(v_1), \ldots, A(v_1)}_{i_1}, \underbrace{A(v_2), \ldots, A(v_2)}_{i_2}, \ldots, \underbrace{A(v_n), \ldots, A(v_n)}_{i_n}) \\ &= q(\underbrace{p_1, \ldots, p_1}_{i_1}, \underbrace{p_2, \ldots, p_2}_{i_2}, \ldots, \underbrace{p_n, \ldots, p_n}_{i_n}),\end{aligned}$$

which completes the proof. □

Claim 6.3 establishes the algebraic relationship between a polynomial's polarization and S-patch control nets for it. Owing to the close connection between geometric constructions and polar forms, the algebraic relationship of Claim 6.3 leads immediately to a geometric construction for an S-patch control net given a Bézier control net for a polynomial surface. This is demonstrated in the following example for a quadratic Bézier triangle:

Example 6.1. As a specific example of the construction of an S-patch control net for a polynomial surface, let Q be a quadratic Bézier triangle with polarization q. The control points for Q on the triangle *rst* are obtained by evaluating q at the points *rst*, as shown in Figure 11. We shall describe the construction of the regular 5-sided S-patch control net for Q on the pentagon *abcde*.

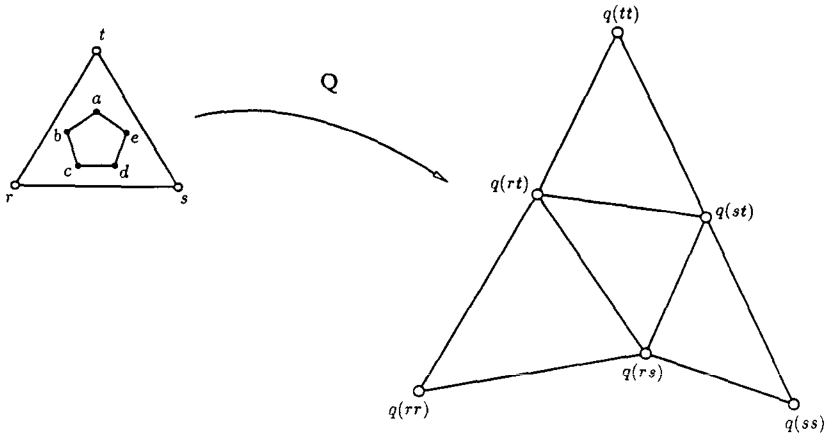

Fig. 11. The domain triangle and control net for a Bézier triangle Q that is to be represented as a regular 5-sided S-patch. Also shown is the domain pentagon for the S-patch.

The first step is to construct the image of *abcde* under the affine map that carries the triangle *rst* onto the triangular "panel" $q(rr)q(rs)q(rt)$. The points thus constructed are the polar values (i.e., values of the polarization) $q(ra)$, $q(rb)$, $q(rc)$, $q(rd)$, and $q(re)$. Using a similar process to find the image of *abcde* on the other two panels results in the situation shown in Figure 12a. Next, find the image of *abcde* under the affine map that carries the triangle *rst* onto the triangle $q(ra)q(sa)q(ta)$, thereby computing the polar values $q(aa)$, $q(ab), \ldots, q(ae)$, as shown in Figure 12b. According to Claim 6.3, the points thus constructed are S-patch control points. The remaining S-patch control points are found by constructing the image of *abcde* on the panels $q(rb)q(sb)q(tb)$, $q(rc)q(sc)q(tc)$, $q(rd)q(sd)q(td)$, and $q(re)q(se)q(te)$, as shown in Figure 12c.

Example 6.2. As another example of S-patch representations of polynomial maps, consider the construction of a regular n-sided depth d S-patch representation of the identity map. That is, we seek control points $\mathbf{P}_{\vec{i}}$ such that

$$p = \sum_{\vec{i}} \mathbf{P}_{\vec{i}} B_{\vec{i}}^{d}(l_1(p), \ldots, l_n(p)).$$

A simple solution to this problem is to construct the d-affine polarization of the identity and then to evaluate it at the locations indicated by Claim 6.3. The d-affine polarization of the identity map is given simply by

$$\frac{u_1 + u_2 + \cdots + u_d}{d}.$$

Evaluating this polar form at the vertices of P as indicated in Claim 6.3, we find that

$$\mathbf{P}_{\vec{i}} = \frac{i_1 p_1 + i_2 p_2 + \cdots + i_n p_n}{d}. \tag{6.3}$$

Examples of control nets produced in this way for various n and d are given in Figure 5.

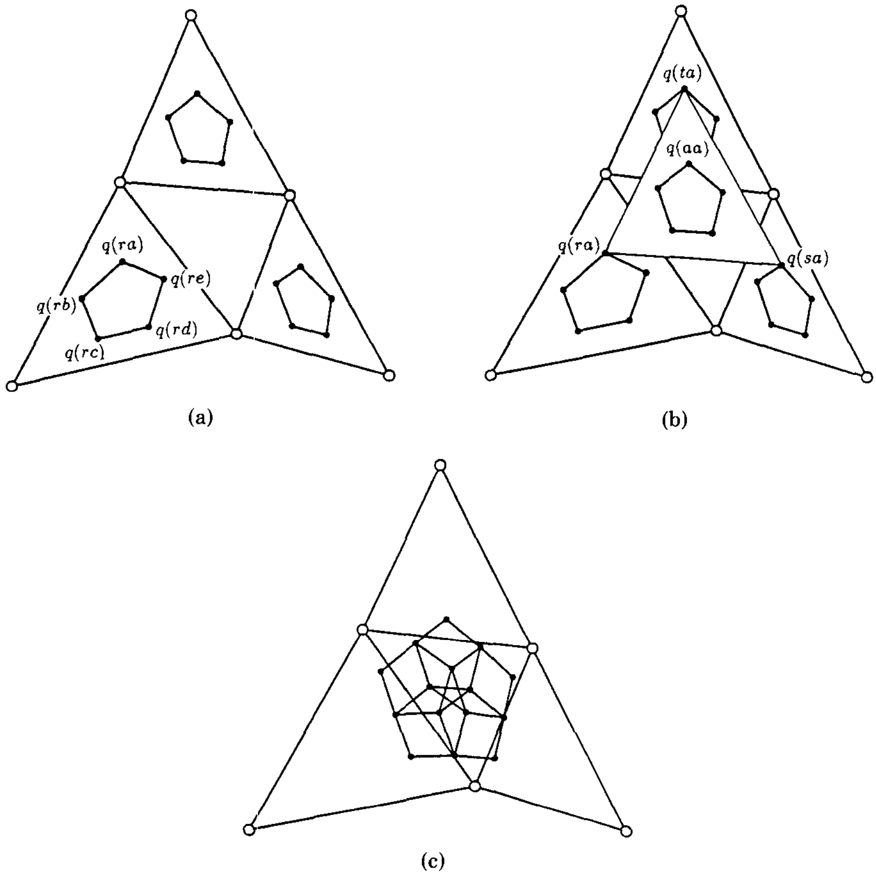

Fig. 12. The construction of a 5-sided regular S-patch control net.

We would now like to generalize Claims 6.2 and 6.3 in a number of ways. First, these claims can be generalized to include the case in which Q is a rational polynomial. The construction of S-patch control nets is very similar in this case, the exception being that the weights take on values other than one and projective images of the polygon are constructed rather than affine images. Second, recall that rational Bézier triangles are identical to 3-sided regular S-patches. The claims can therefore be interpreted as stating that 3-sided regular S-patches can be represented as n-sided regular S-patches. One might conjecture that a similar result is more generally true for the case in which an m-sided regular S-patch is to be represented as an n-sided regular S-patch. This conjecture holds, as we now show. Moreover, the proof is constructive in that it provides an algorithm for computing the n-sided representation given the m-sided representation.

CLAIM 6.4. *For every m-sided regular S-patch of depth d, there exists an equivalent n-sided regular S-patch of depth $d(m-2)$. In other words, the space of m-sided regular S-patches of depth d is contained in the space of n-sided regular S-patches of depth $d(m-2)$.*

Table I. Corollaries of Claim 6.4

m	n	Interpretation
3	4	Triangle → Tensor product
4	3	Tensor product → Triangle
3	n	Triangle → S-patch
4	n	Tensor product → S-patch
m	3	S-patch → Triangle
m	4	S-patch → Tensor product

PROOF. Let L_i denote the embedding L for an i-sided S-patch, let A_i denote the affine map with respect to which L_i is pseudoaffine, and let I denote the identity mapping on the domain space $\mathscr{X}$. Also, denote by $S = \mathbf{B}_m \circ L_m$ the m-sided S-patch for which an n-sided representation is to be constructed. The proof proceeds by using essentially the same reasoning as was used in the proof of Claim 6.2:

$$\begin{aligned} S &= \mathbf{B}_m \circ L_m \\ &= \mathbf{B}_m \circ L_m \circ I \\ &= \mathbf{B}_m \circ L_m \circ (A_n \circ L_n) \\ &= (\mathbf{B}_m \circ L_m \circ A_n) \circ L_n. \end{aligned}$$

The term in parentheses consists of the composition of three rational polynomial maps. Control nets for $\mathbf{B}_m$ and A_n are already known, and the control net for L_m can be obtained by evaluating its multiprojective polarization. A slight generalization of the Bézier simplex composition algorithm developed in [6] can therefore be used to compute the control points for the map $\mathbf{B}_n := \mathbf{B}_m \circ L_m \circ A_n$ [8]. This definition of $\mathbf{B}_n$ allows S to be written as $S = \mathbf{B}_n \circ L_n$, which is an n-sided S-patch representation. Since $\mathbf{B}_m$ is of degree d, L_m is of degree $m - 2$, and since A_m is of degree 1, $\mathbf{B}_n$ is of degree $d(m - 2)$, implying that $S = \mathbf{B}_n \circ L_n$ is an S-patch representation of depth $d(m - 2)$. □

Claim 6.4 has a number of corollaries, one of which is Claim 6.2. Other corollaries can be interpreted as change of representation algorithms; these are summarized in Table I.

6.5 Nonparametric S-Patches

The coefficients of a real-valued polynomial expressed in Bernstein form, also known as Bézier ordinates [12, 13], have a simple geometric interpretation. In particular, they are closely related to the geometric locations of the triangular Bézier control points for the graph of the polynomial. As a direct consequence of the pseudoaffine property of Section 6.2, a similar results holds more generally for real-valued functions given in regular S-patch form when the rational weights are set to one. Suppose that $F: P \to \mathbf{R}$ is a real-valued function given in regular S-patch form as

$$F(p) = \sum_{\vec{i}} f_{\vec{i}} B^d_{\vec{i}}(l_1(p), \ldots, l_n(p)).$$

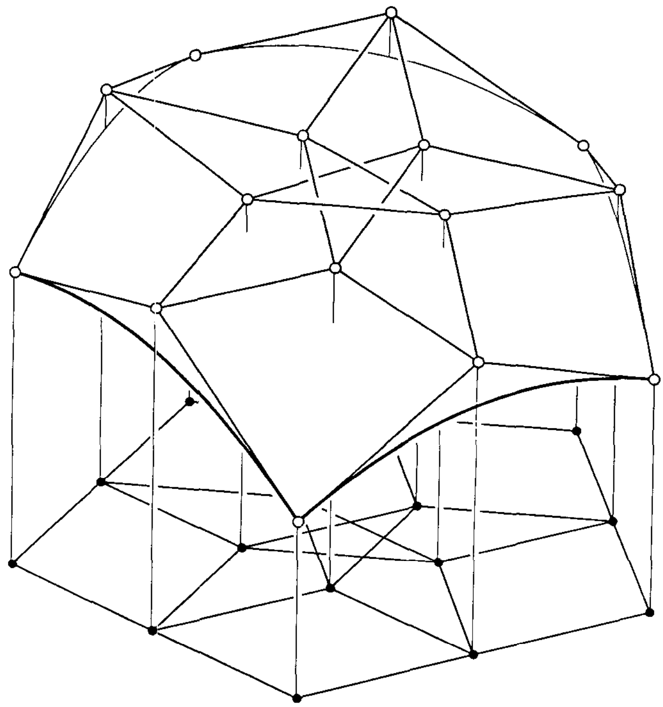

Fig. 13. The graph of a depth 2 5-sided function in regular S-patch form.

The graph of F is the parametric function $G_F(p) = (p, F(p))$. The S-patch control points $\mathbf{G}_{\bar{i}}$ of G_F must therefore be such that the first component represents the identity map and the last component represents F. Using the results of Example 6.2, these control points are therefore given by

$$\mathbf{G}_{\bar{i}} = \left(\frac{i_1 p_1 + \cdots + i_n p_n}{d}, f_{\bar{i}} \right).$$

Figure 13 shows the graph of a depth 2 5-sided function.

7. JOINING REGULAR S-PATCHES TO BÉZIER TRIANGLES

Using Claim 6.3 for representing polynomials in S-patch form, it is a simple matter to derive an algorithm for smoothly joining (in a C^k sense) regular S-patches to Bézier triangles. To do this, suppose that Q is the Bézier triangle to be joined to with C^k continuity, let T denote Q's domain triangle, and let q denote Q's polarization. The algorithm consists of the following steps:

(1) Using Claim 6.3, compute the S-patch control net for Q defined on an adjacent domain polygon P. The S-patch thus constructed meets Q with C^∞ continuity since they represent the same function.
(2) If the S-patch control points within k vertices of the boundary are kept fixed, the first k derivatives of the S-patch remain equal to Q's derivatives, and therefore the S-patch and Q meet C^k.

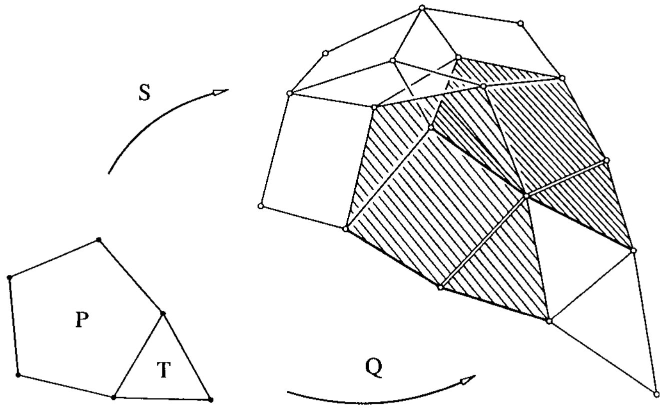

Fig. 14. C^1 **joining of a regular S-patch to a Bézier triangle.**

Fig. 15. A degree 2 Bézier triangle and a 5-sided, depth 2 S-patch meeting with C^1 continuity.

The geometric interpretation of this construction for C^1 is shown in Figure 14. Note that adjacent panels must be affine images of the domain polygons and hence are coplanar. Figure 15 shows an example of this method for a degree 2 Bézier triangle joined in a C^1 fashion to a 5-sided, depth 2 S-patch.

A slight generalization can be used to achieve G^k continuity (cf. [5] and [18]), assuming that there exists a construction for joining Bézier triangles together with G^k continuity. (Farin [10] and Piper [21], for instance, have exhibited such constructions for $k = 1$.) This hypothesized construction can be used as follows to achieve a G^k join of an S-patch to a Bézier triangle Q:

(1) Use the hypothesized construction to determine a Bézier triangle $\tilde{Q}$ that meets Q with G^k continuity.
(2) Use Claim 6.3 to compute the S-patch control net for $\tilde{Q}$. The resulting S-patch also meets Q with G^k continuity.
(3) The S-patch control points further than k vertices from the boundary can be moved at will without destroying the G^k join.

The important aspect of this result is that a pair of S-patches are no more difficult to join together than a pair of Bézier triangles. Since S-patches in general have more control points influencing derivatives across boundaries than do equal-depth Bézier triangles, more general G^k joins may be possible. Further work in this direction is needed.

8. SUMMARY

In this paper we have introduced a new class of surface representations, called S-patches, that may be defined on arbitrary convex polygonal domains. Based on the idea of restricting Bézier simplexes to embedded surfaces, the theory of S-patches can be derived largely by adapting results from the theory of multivariate Bernstein–Bézier representations. Using this technique, we have shown that S-patches can be geometrically constructed, that they possess a depth elevation algorithm, that they lie in the convex hull of their defining points, and that the positional and derivative behavior of their boundary curves is determined entirely by control points "near" the boundary.

It was shown that regular S-patches, that is, S-patches defined on regular polygonal domains, possess additional special properties. In particular, it was shown that regular S-patches unify the theory of Bézier triangles and bi-d-ic tensor product Bézier surfaces; it was also shown that regular S-patches can be joined to Bézier triangles with either C^k continuity for arbitrary k, or G^1 continuity. However, it appears unlikely that regular S-patches possess a recursive subdivision algorithm.

Quite a lot of work remains to be done to fully develop the theory of S-patches. Here we list a number of topics for future research:

Linear independence. We have shown that regular S-patch blending functions are not necessarily linearly independent. In particular, linear dependence of the blending functions was shown to occur for parallelogram domains. It is desirable to know exactly when S-patch basis functions are linearly independent.

Pseudoaffine embeddings on irregular domains. The pseudoaffine property has been shown to be very useful in developing algorithms for representing polynomials and for joining polynomials and S-patches. However, the embedding (L from eq. (3.4)) we have used in this paper is pseudoaffine only when the domain polygon is regular. If pseudoaffine embeddings can be constructed on arbitrary convex polygons, many of the results in this paper could be immediately extended. The use of piecewise smooth embeddings can also be considered.

Smooth interpolation to scattered data. The problem that originally motivated the development of S-patches is that of constructing smooth surfaces that interpolate the vertices of an arbitrary polyhedron. This problem has been previously addressed by a number of authors for the case in which the vertices of the polyhedron are interpolated using only triangular and/or quadrilateral patches (cf. [3], [11], [20], [21], and [26]). We are currently developing a scheme that uses S-patch representations to construct surfaces given polyhedrons whose faces have any number of sides.

Derivatives of S-patches. Detailed knowledge of derivative behavior at the boundaries and over the interior of surface patches is important for constructions ensuring geometric continuity, as well as for high-quality surface-shading algorithms. The compositional structure of S-patches allows these derivatives to be studied using the chain rule. That is, an S-patch $S = \mathbf{B} \circ E$ has a differential given by $DS = D\mathbf{B} \circ DE$. Thus, knowledge of S-patch derivative behavior can be determined once the differentials of $\mathbf{B}$ and E are known. The joining of patches with geometric continuity is not only of theoretical interest, it is necessary for developing effective solutions to the scattered data interpolation problem.

APPENDIX A. Proof of Claim 6.1

The proof proceeds by showing that $A \circ L$ is the identity map when restricted to an edge of the domain polygon P. We can then use degree arguments to show that $A \circ L$ must be the identity everywhere. Before proving the claim, a few preparatory lemmas are in order.

LEMMA A.1. *If $f\colon \mathbf{R}^2 \to \mathbf{R}$ is a polynomial map of degree less than or equal to d that vanishes on the line $g(x, y) = 0$, then g divides f.*

PROOF. Set up a coordinate system (x', y') so that the x' axis coincides with the line $g(x, y) = 0$. In the primed system, g can be expressed as

$$g(x', y') = ay'$$

where a is a constant, and f can be expressed as

$$f(x', y') = p_0(x') + p_1(x')y' + p_2(x')y'^2 + \cdots + p_d(x')y'^d$$

where $p_0, \ldots, p_d$ are univariate polynomials. Since f vanishes when g does, the polynomial $p_0(x')$ must be identically zero. Thus, f can be written as

$$\begin{aligned} f(x', y') &= y'[p_1(x') + p_2(x')y' + \cdots + p_d(x')y'^{d-1}] \\ &= \frac{1}{a} g(x', y')[p_1(x') + p_2(x')y' + \cdots + p_d(x')y'^{d-1}], \end{aligned}$$

showing that g does in fact divide f. □

LEMMA A.2. *Let ϕ be an affine functional defined on an affine plane that vanishes at the points P_1 and P_2. If Q_1 and Q_2 are two points on a line parallel to P_1P_2, then $\phi(Q_1) = \phi(Q_2)$.*

PROOF. If Q_1 and Q_2 lie on the line P_1P_2, the lemma is trivially true. Otherwise, write Q_2 barycentrically with respect to the triangle $P_1P_2Q_1$ and use the fact that ϕ is an affine map. □

LEMMA A.3. *The restriction of L to an edge of P is a pseudoaffine map with respect to A whenever P is regular.*

PROOF. If $n = 3$, L is everywhere affine as shown in Section 3, so its restriction to each edge is affine. If $n > 3$, consider the restriction L_e of L to the edge p_1p_2 (the other edges follow from symmetry). Referring to eq. (3.5), L_e will be of the form

$$L_e(p) = l_1(p)v_1 + l_2(p)v_2, \qquad p \in p_1p_2.$$

The composition map $A \circ L_e$ is therefore of the form

$$\begin{aligned} A \circ L_e(p) &= A(l_1(p)v_1 + l_2(p)v_2) \\ &= l_1(p)A(v_1) + l_2(p)A(v_2) \\ &= l_1(p)p_1 + l_2(p)p_2 \\ &= \frac{\pi_1(p)p_1 + \pi_2(p)p_2}{\pi_1(p) + \pi_2(p)}. \end{aligned}$$

The functionals π_1 and π_2 share the product $\alpha_3 \cdots \alpha_{n-1}$ as a common factor. Since this common factor never vanishes on p_1p_2, it can be divided out, leaving

$$A \circ L_e(p) = \frac{\alpha_2(p)p_1 + \alpha_n(p)p_2}{\alpha_2(p) + \alpha_n(p)}, \qquad p \in p_1p_2.$$

In this form, we recognize that $A \circ L_e$ is a projective map from the line p_1p_2 onto itself. We can show that this is the identity map by showing that it fixes three points on the line. It is particularly easy to show that two points, namely, p_1 and p_2, are fixed: The point p_1 is fixed under $A \circ L_e$ since α_n vanishes at p_1; a similar argument holds for p_2 since α_2 vanishes at p_2. Showing fixture of a third point requires us to use regularity of the domain polygon P. First, recall that $\alpha_2(p_4) = 1$. If P is regular, the the line p_1p_4 is parallel to p_2p_3. By Lemma A.2, we conclude that $\alpha_2(p_1) = 1$. With these simple facts, fixture of the midpoint follows readily:

$$\begin{aligned} A \circ L_e\left(\frac{p_1 + p_2}{2}\right) &= \frac{\alpha_2\left(\frac{p_1 + p_2}{2}\right)p_1 + \alpha_n\left(\frac{p_1 + p_2}{2}\right)p_2}{\alpha_2\left(\frac{p_1 + p_2}{2}\right) + \alpha_n\left(\frac{p_1 + p_2}{2}\right)} \\ &= \frac{\frac{\alpha_2(p_1) + \alpha_2(p_2)}{2}p_1 + \frac{\alpha_n(p_1) + \alpha_n(p_2)}{2}p_2}{\frac{\alpha_2(p_1) + \alpha_2(p_2)}{2} + \frac{\alpha_n(p_1) + \alpha_n(p_2)}{2}} \\ &= \frac{p_1 + p_2}{2}. \end{aligned}$$

□

We are now in a position to prove the claim.

PROOF OF CLAIM 6.1. Consider the following map H that carries points in $\mathscr{X}$ into vectors in $\mathscr{X}$:

$$H(p) = (A \circ L(p) - p)(\pi_1(p) + \cdots + \pi_n(p)). \tag{A.1}$$

If we establish a coordinate system on $\mathscr{X}$, then H is represented by two functions Hx, Hy, each of which maps $\mathbf{R}^2$ into $\mathbf{R}$. Since the second factor of eq. (A.1) cancels the denominator of L, Hx and Hy are (nonrational) polynomials. They are each of degree $n - 1$ since p (represented by the polynomials x and y) is a linear polynomial and the second factor of eq. (A.1) is a polynomial of degree $n - 2$. By Lemma A.3, $H(p)$ is the zero vector whenever p is on an edge of P. Thus, Hx and Hy each vanish on the n lines defined by $\alpha_1(p) = 0, \ldots, \alpha_n(p) = 0$. By Lemma A.1, the functions Hx and Hy must therefore be divisible by n linear factors. Since they are polynomials of degree $n - 1$, the only way that they can have n linear factors is if they identically vanish. Thus, $Hx(x, y) = 0$ and $Hy(x, y) = 0$, implying that $H(p)$ is identically the zero vector.

The proof is completed by noting that if $p \in P$ then the second factor of eq. (A.1) is strictly positive, implying that $A \circ L(p) - p$ is the zero vector for all $p \in P$; thus, $A \circ L(p) = p$ for all $p \in P$. Since $A \circ L$ is a rational polynomial map shown to be the identity on an open set, it must be the identity everywhere. □

ACKNOWLEDGMENTS

The authors would like to thank Michael Lounsbery, James King, and the other members of the CAGD seminar at the University of Washington for their help in developing the ideas contained herein. Gemini Lasswell deserves special thanks for her help in software development, image generation, and proofreading.

REFERENCES

1. BOEHM, W., FARIN, G., AND KAHMANN, J. A survey of curve and surface methods in CAGD. *Comput. Aided Geom. Des. 1*, 1 (July 1984), 1–60.
2. CHARROT, P., AND GREGORY, J. A. A pentagonal surface patch for computer aided geometric design. *Comput. Aided Geom. Des. 1*, 1 (July 1984), 87–94.
3. CHIYOKURA, H., AND KIMURA, F. Design of solids with free-form surfaces. *Comput. Graph. 17*, 3 (July 1983), 289–298.
4. DE BOOR, C. B-form basics. In *Geometric Modeling: Algorithms and New Trends*, G. Farin, Ed. SIAM, Philadelphia, Pa., 1987, pp. 131–148.
5. DEROSE, T. D. Geometric continuity: A parametrization independent measure of continuity for computer aided geometric design. Ph.D. thesis, Dept. of Electrical Engineering and Computer Science, Univ. of California, Berkeley, Aug. 1985. (Also available as Tech. Rep. UCB/CSD 86/255, Computer Sciences Division, Dept. of Electrical Engineering and Computer Sciences, Univ. of California, Berkeley.)
6. DEROSE, T. D. Composing Bézier simplexes. *ACM Trans. Graph. 7*, 3 (July 1988), 198–221.
7. DEROSE, T. D. Geometric programming: A coordinate-free approach. In *SIGGRAPH 88 Tutorial Course Notes*, Course No. 25, ACM, New York, Aug. 1988.
8. DEROSE, T. D., GOLDMAN, R. N., HAGEN, H., AND MANN, S. Composing rational B-splines. In preparation.
9. DODSON, C. T. J., AND POSTON, T. *Tensor Geometry: The Geometric Viewpoint and Its Uses.* Paperback ed. Pitman, London, 1979.
10. FARIN, G. A construction for visual C^1 continuity of polynomial surface patches. *Comput. Graph. Image Process. 20*, 3 (Nov. 1982), 272–282.
11. FARIN, G. Smooth interpolation to scattered 3D data. In *Surfaces in CAGD*, R. E. Barnhill and W. Boehm, Eds. North-Holland, Amsterdam, 1983, pp. 43–63.
12. FARIN, G. Triangular Bernstein–Bézier patches. *Comput. Aided Geom. Des. 3*, 2 (Aug. 1986), 83–127.
13. FARIN, G. *Curves and Surfaces for Computer Aided Geometric Design: A Practical Guide.* Academic Press, New York, 1988.
14. GREGORY, J. A. C^1 rectangular and non-rectangular surface patches. In *Surfaces and CAGD*, R. E. Barnhill and W. Boehm, Eds. North-Holland, Amsterdam, 1983, pp. 25–33.

15. GREGORY, J. A. *N*-sided surface patches. In *Mathematics of Surfaces*, J. Gregory, Ed. Clarendon Press, Oxford, England, 1986, pp. 217–232.
16. GREGORY, J. A., AND HAHN, J. Geometric continuity and convex combination patches. *Comput. Aided Geom. Des. 4*, 1–2 (July 1987), 79–90.
17. HERRON, G. J. Triangular and multisided patch schemes. Ph.D. thesis, Dept. of Mathematics, Univ. of Utah, Salt Lake City, 1979.
18. HERRON, G. J. Techniques for visual continuity. In *Geometric Modeling: Algorithms and New Trends*, G. Farin, Ed. SIAM, Philadelphia, Pa., 1987, pp.163–174.
19. HOSAKA, M., AND KIMURA, F. Non-four-sided patches expressions with control points. *Comput. Aided Geom. Des. 1*, 1 (July 1984), 75–86.
20. JENSEN, T. Assembling triangular and rectangular patches and multivariate splines. In *Geometric Modeling: Algorithms and New Trends,* G. Farin, Ed. SIAM, Philadelphia, Pa., 1987, pp. 203–220.
21. PIPER, B. R. Visually smooth interpolation with triangular Bézier patches. In *Geometric Modeling: Algorithms and New Trends*, G. Farin, Ed. SIAM, Philadelphia, Pa., 1987, pp. 221–233.
22. RAMSHAW, L. Blossoming: A connect-the-dots approach to splines. Res. Rep. 19, Digital Equipment Corp Systems Research Center, Palo Alto, Calif., June 21, 1987.
23. RAMSHAW, L. Béziers and B-splines as multiaffine maps. In *Theoretical Foundations of Computer Graphics and CAD,* R. A. Earnshaw, Ed. NATO ASI Series, vol. F40, Springer-Verlag, New York, 1988, pp. 757–776.
24. RAMSHAW, L. Blossoms are polar forms. Res. Rep. 34, Digital Equipment Corp Systems Research Center, Palo Alto, Calif., Jan. 1989.
25. SABIN, M. A. Non-rectangular surface patches suitable for inclusion in a B-spline surface. In *Proceedings of Eurographics '83*, P. ten Hagen, Ed. North-Holland, Amsterdam, 1983, pp. 57–69.
26. SHIRMAN, L. A., AND SÉQUIN, C. H. Local surface interpolation with Bézier patches. *Comput. Aided Geom. Des. 4*, 4 (Dec. 1987), 279–295.
27. VARADY, T. Survey and new results in *n*-sided patch generation. In *The Mathematics of Surfaces II*, R. R. Martin, Ed. Clarendon Press, Oxford, England, 1987, pp. 203–236.

Received August 1988; revised February 1988; accepted February 1988